JOURNAL OF MATERIALS SCIENCE 16 (1981) 809–812

Mechanical properties of sintered hydroxyapatite for prosthetic applications

M. AKAO
Dental Technology, Faculty of Dentistry, Tokyo Medical and Dental University, Yushima, Bunkyo, Tokyo 113, Japan

H. AOKI, K. KATO
Institute for Medical and Dental Engineering, Tokyo Medical and Dental University, Kanda Surugadai, Chiyoda, Tokyo 101, Japan

The compressive, flexural, torsional and dynamic torsional strengths of polycrystalline hydroxyapatite sintered at a temperature of 1300° C for 3 h were found to be 509, 113, 76 and 68 MPa, respectively. The mechanical properties of polycrystalline hydroxyapatite are compared with those of cortical bone, dentine and enamel. SEM observation of the fracture surfaces indicates a predomination of transgranular failures.

1. Introduction

Several workers [1–3] have attempted to develop bone and tooth implant materials composed of polycrystalline hydroxyapatite. The chemical and crystallographic properties of polycrystalline hydroxyapatite closely resemble those of bone and tooth minerals, and the sintered material has superior compatibility with these tissues. The brittle nature of the ceramic restricts the clinical orthopedic and dental applications. Rao and Boehm [4] reported the compressive strength of sintered hydroxyapatite; Jarcho *et al.* [5] measured the compressive and flexural strengths. In the present study, the compressive, flexural, torsional and dynamic torsional strengths of polycrystalline hydroxyapatite were estimated and compared with those of cortical bone, dentine and enamel.

2. Experimental procedure

2.1. Preparation of sintered hydroxyapatite

A suspension of 0.5 M $Ca(OH)_2$ in 1000 ml distilled water was vigorously stirred and a solution of 0.3 M H_3PO_4 in 1000 ml distilled water was slowly added as drops over 1 to 2 h under a condition of pH > 7 to produce a gelatinous precipitate. The reaction mixture was stirred for a few hours and aged at room temperature for a week. The resulting slurry was filtrated. The filter cake was dried at 80° C and calcined at 800° C for 3 h. The product has a Ca/P ratio of 1.69 estimated by standard EDTA titration for Ca and phosphomolybdate techniques for PO_4. The finely ground powder, mixed with 1 wt% cornstarch and a few drops of water, was pressed by a mould at a pressure of 60–80 MPa. The compact was heated in air at 1150, 1200, 1250 and 1300° C for 3 h. In the X-ray powder diffraction patterns, α- and β-$Ca_3(PO_4)_2$ phases were not detected; the maximum sensitivity for detection was 2% in these systems. The porosity values were calculated by assuming the theoretical density of 3.16 g cm^{-3}. The average grain sizes (see Table I) were estimated by the linear intercept method from scanning electron micrographs of the specimens after etching in 0.1 M acetic acid solution for 5 min.

2.2. Material testing

Test samples of the sintered hydroxyapatite were cut from discs with a low-speed diamond saw and

TABLE I Porosity and grain size results for sintered hydroxyapatite

Temperature (°C)	Time (h)	Porosity (%)	Grain size (μm)
1150	3	19.4	1.04 ± 0.46
1200	3	9.1	1.32 ± 0.61
1250	3	3.9	2.03 ± 0.91
1300	3	2.8	3.40 ± 1.01

0022–2461/81/030809–04$02.40/0

polished before testing with 800-grit SiC. The compression test was performed on a bar of dimensions 5mm x 5 mm x 10 mm at a crosshead speed of 2.0 mm min^{-1}; the 3-point bending test was performed on a 15 mm span of bar 2 mm x 4 mm in cross-section at a crosshead speed of 0.5 mm min^{-1}; the torsional tests were performed on bars 5 mm x 5 mm in cross-section at a torsion speed of 0.21 rad sec^{-1} for static test and a torsion speed of 7.85 rad sec^{-1} with an impact energy of 0.074 Nm for dynamic test. For each test the number of specimens tested was between 20 and 30. The displacement values in the 3-point bending and compression tests were measured by a differential transformer. A load–deflection curve plotted from the results of the 3-point bending test is shown in Fig. 1. The fracture surfaces in the bending and torsional failures were investigated by SEM techniques.

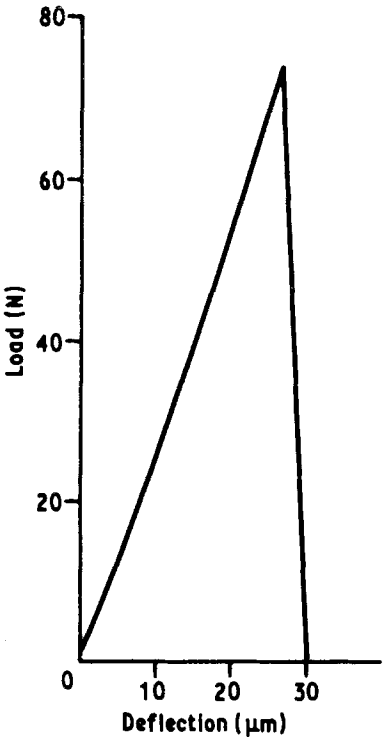

Figure 1 A load–deflection curve plotted from results of a 3-point bending test for sintered hydroxyapatite.

3. Results and discussion

3.1. Mechanical properties

The results are summarized in Table II. The mechanical properties of the materials sintered at 1150° C with about 20% porosity were very low. The maximum compressive, flexural and static torsional strengths were observed at 1300° C. The strength of brittle polycrystalline materials depends on porosity and grain size [6]. Rao and Boehm [4] have reported that the compressive strength of apatite has an exponential dependence on porosity. The flexural strengths of the materials measured in this work tended to depend on porosity rather than grain size.

Rao and Boehm [4] reported the compressive strengths of hydroxyapatite made by sintering of pressed powders prepared from $CaCO_3$ and H_3PO_4; the strengths ranged from 13.8 to 207 MPa. Jarcho *et al.* [5] measured the compressive and flexural strengths of dense polycrystalline hydroxyapatite obtained by heating the gelatinous precipitate prepared from $Ca(NO_3)_2 \cdot 4H_2O$ and $(NH_4)_2HPO_4$. The compressive strength of the latter material (917 MPa) is greater than that measured for the present materials.

Jarcho *et al.* [5] reported that the flexural strengths measured on bars of dimensions 2 mm x 2 mm x 30 mm and of unknown span were 111.7 MPa for as-cut specimens and 195.8 MPa for specimens polished using a 1 μm diamond paste. It is difficult to compare flexural strengths measured by different techniques, because the flexural strength largely depends on the surface condition and grain size. In order that a comparison could be made, polycrystalline hydroxyapatite was prepared by the method described by Jarcho *et al.* [5]. The product contained 2 wt% α-$Ca_3(PO_4)_2$ and the average grain size was

TABLE II Compressive, flexural, torsional and dynamic torsional strengths, and moduli of elasticity in compression and bending, for sintered hydroxyapatite

Temperature (°C)	Compressive strength σ_C (MPa)	Flexural strength σ_F (MPa)	Torsional strength τ_{ST} (MPa)	Dynamic torsional strength τ_{DY} (MPa)	Modulus of elasticity in compression E_C (GPa)	Modulus of elasticity in bending E_B (GPa)
1150	308 ± 46	61 ± 8	50 ± 7	57 ± 6	42.2 ± 3.8	44.3 ± 3.5
1200	415 ± 46	104 ± 11	62 ± 5	92 ± 6	74.6 ± 4.1	80.0 ± 6.4
1250	465 ± 58	106 ± 10	75 ± 4	76 ± 5	79.0 ± 4.8	85.1 ± 6.1
1300	509 ± 57	113 ± 12	76 ± 5	68 ± 5	81.4 ± 4.6	87.8 ± 6.0

TABLE III Mechanical properties of various hard tissues and references

Material	Compressive strength (MPa)	Tensile strength (MPa)	Modulus of elasticity (GPa)
Cortical bone	88.3–163.8 [7]	88.9–113.8 [8]	3.88–11.7 [7]
Dentine	295 [10]	51.7 [9]	18.2 [10]
Enamel	384 [10]	10.3 [9]	82.4 [10]

$0.63 \pm 0.35\,\mu m$. The average flexural strength for 15 specimens measured by the method given in Section 2.2. was 168 ± 22 MPa; the modulus of elasticity in bending measured was 103 ± 7 GPa. This flexural strength is greater than that of the materials prepared as in Section 2.1., the results of which are shown in Table II. This is because the specimens prepared as in [5] are of a finer grain size; this modulus of elasticity is greater than that in tension (34.5 GPa) measured by Jarcho *et al.* [5], and is greater than those measured for the present materials (see Table II) probably as a result of the finer grain size. The moduli of elasticity in bending for the present materials tended to be greater than that measured in compression testing, as shown in Table II.

3.2. Comparison of the mechanical properties to various hard tissues

The mechanical properties of cortical bone, dentine and enamel [7–10] are listed in Table III. Note that the strength of cortical bone depends both on the degree of calcification and on fibre orientation [7, 8]. Static and dynamic torsional strengths of ox femoral cortex, measured by the method given in Section 2.2, where 52 ± 5 and 59 ± 7 MPa, respectively.

The compressive strength of the sintered hydroxyapatite is approximately 3 to 6 times as strong as that of cortical bone, and is very roughly 1.5 times as strong as those of dentine and enamel. The flexural strength of sintered hydroxyapatite is very similar to the tensile strength of cortical bone, and is 2 and 10 times as strong as the tensile strengths of dentine and enamel respectively. The static and dynamic torsional strengths of hydroxyapatite are about 1.5 times as strong as those of cortical bone. The value of the modulus of elasticity is between 5 and 20 times as large as that of cortical bone and is about 5 times as large as that of dentine. The modulus of elasticity for the present hydroxyapatite is in close agreement with that of enamel which is composed of 98 wt% hydroxyapatite. The sintered hydroxyapatite has sufficiently good mechanical properties to be utilized as bone and tooth implant materials with superior bio-compatibility.

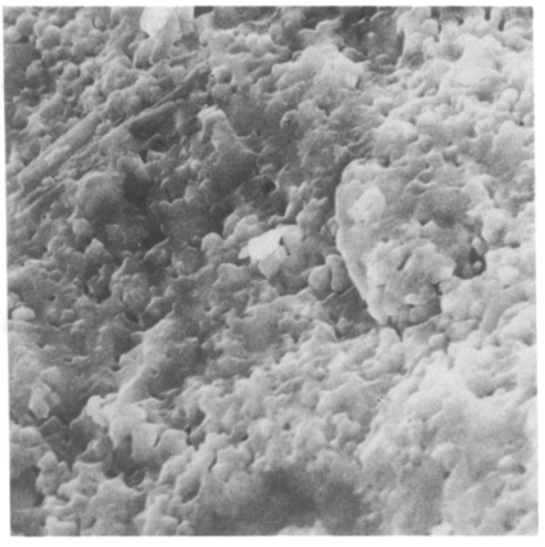

Figure 2 Scanning electron micrograph of static torsion fracture surface of hydroxyapatite sintered at 1200° C for 3 h, showing intergranular fracture (× 3000).

3.3. Fracture topography

SEM examination of fracture surfaces due to the flexural and torsional failures revealed that the fracture of the specimens with 2 to 4% porosity occurs mainly as a transgranular fracture process while that of the specimens with 9 to 20% porosity occurs mainly as an intergranular fracture process. A static torsion fracture surface of a specimen sintered at 1200° C is shown in Fig. 2. Intergranular fractures and a few grain-boundary pores are visible. Fig. 3 shows the fracture surface of a specimen sintered at 1300° C. Transgranular fracture is predominant and minor intergranular fracture is observed around the grain-boundary pores.

A pattern, similar to that shown in Fig. 4, was frequently observed in the static and dynamic torsion fracture surfaces of the specimens sintered at 1250 and 1300° C. The pattern is similar to the ripple and wave patterns observed in the fracture surface of pure metals described by Beachem and Meyn [11]. It is interesting that the fracture surfaces of brittle polycrystalline hydroxyapatite closely resemble the slip patterns of ductile pure metals.

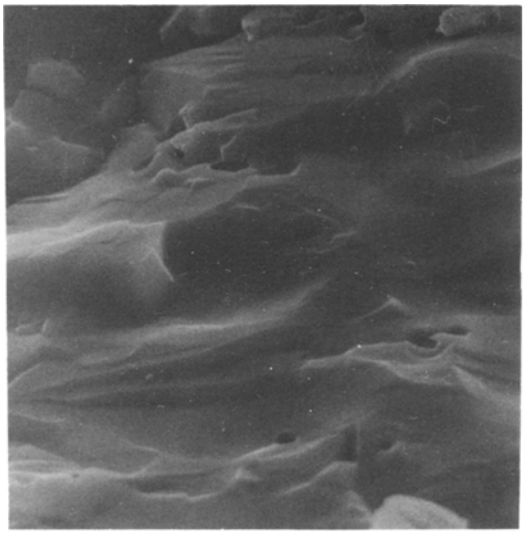

Figure 3 Scanning electron micrograph of static torsion fracture surface of hydroxyapatite sintered at 1300° C for 3 h showing transgranular fracture (× 3000).

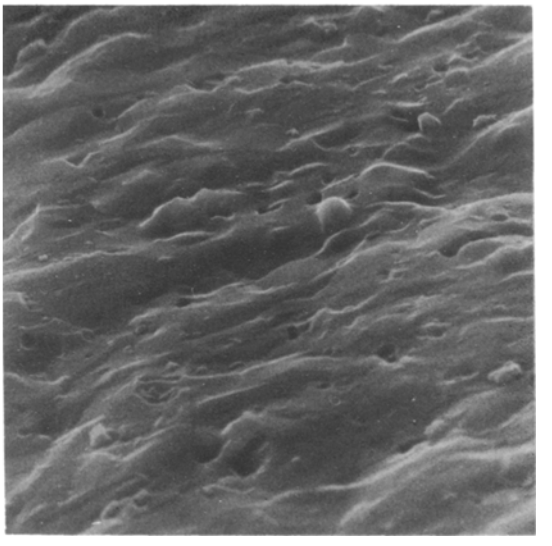

Figure 4 Scanning electron micrograph of static torsion fracture surface of hydroxyapatite sintered at 1250° C for 3 h showing the ripple pattern (× 3000).

Acknowledgements

We are grateful to Professor A. Muramastu, Tokyo Medical and Dental University, and Dr M. Iida, Kakeyu Rehabilitation Research Centre, for their permission to use their testing machines.

References

1. E. B. NERY, K. L. LYNCH, W. M. HIRTE and K. H. MULLER, *J. Periodontol.* **46** (1975) 328.
2. H. AOKI, K. KATO and T. TABATA, *Rep. Inst. Med. Dent. Eng. Japan* **11** (1977) 33.
3. M. JARCHO, J. F. KAY, K. I. GUMAER, R. H. DOREMUS and H. P. DROBECK, *J. Bioeng.* **1** (1977) 79.
4. W. R. RAO and R. F. BOEHM, *J. Dent. Res.* **53** (1974) 1351.
5. M. JARCHO, C. H. BOLEN, M. B. THOMAS, J. BOBICK, J. F. KAY and R. H. DOREMUS, *J. Mater. Sci.* **11** (1976) 2027.
6. F. P. KNUDSEN, *J. Amer. Ceram. Soc.* **42** (1959) 376.
7. A. ASCENZI and E. BONUCCI, *Anat. Rec.* **158** (1967) 375.
8. *Idem, ibid.* **161** (1968) 377.
9. R. L. BOWEN and M. S. RODRIGUEZ, *J. Amer. Dent. Assoc.* **64** (1962) 378.
10. F. A. PEYTON, *Ann. New York Acad. Sci.* **146** (1968) 96.
11. C. D. BEACHEM and D. A. MEYN, *ASTM STP* **436** (1968) 59.

Received 15 May and accepted 2 September 1980.